

Exploring nonlinearities in a positive ion-negative ion (PINI) plasma: can other processes mimic debris-induced effects?

Hitendra Sarkar and Madhurjya P. Bora^a

Physics Department, Gauhati University, Guwahati 781014, India

In this work, an analysis of nonlinear waves and structures induced by an external charged debris in a positive ion-negative ion (PINI) plasma is presented. The results obtained are compared with findings from available experiments involving PINI plasma. The process of formation of different nonlinear structures is examined theoretically through a forced Korteweg-de Vries (fKdV) equation, which is also verified with a multi-fluid flux-corrected transport simulation code (mFCT). Various processes which are responsible for different nonlinear waves and structures excited by differently charged external debris are pointed out. This work also points out the similarities in different nonlinear structures excited by an external charged debris and the underlying processes (this work) and those observed experimentally through processes that do not involve any external debris.

I. INTRODUCTION

Nonlinear waves ubiquitously drive the dynamics of nature's most intricate systems, shaping complex phenomena from plasma instabilities to oceanic rogue waves in ways both beautiful and unpredictable. Plasma solitons and shocks remain prime examples of such structures that govern the energy transport and wave dynamics both in laboratory and astrophysical environments. Solitons or solitary waves can be considered as localized compressions or rarefactions of plasma densities arising out of the interplay between nonlinearity and dispersion. On the contrary, shock waves are usually associated with some dissipation mechanisms such as kinematic viscosity, Landau damping, and collision among ions and neutrals along with inherent nonlinearity, dispersion, and weak dissipation. During the nonlinear evolution of ion-acoustic wave (IAW) in a dissipative plasma, the leading edge of a propagating wave gets steepened as dissipation dominates over dispersion and a shock front is formed. In contrast to this, in a collision-less dispersive fluid, shock waves can form without dissipation and often have an oscillatory signature and are known as dispersive shock waves (DSWs) [1–4]. Nevertheless, the nature of these nonlinear structures is largely determined by the background plasma conditions, constituents, and the associated physical parameters.

The characteristics of ion-acoustic solitons or shock waves in a usual electron-ion ($e-i$) plasma are significantly different from that of a multi-ion plasma such as a positive ion-negative ion (PINI) plasma [5–8]. In fact, an $e-i$ plasma can only support compressive solitons with positive electrostatic potential. However, with an addition of even a small amount of one or more extra ion species to the plasma, drastically changes the dynamics of the plasma. It is observed that in a multicomponent plasma, the IAW propagation is mainly influenced by the lighter ions and changes in their concentrations and temperatures may lead to substantial modification of the wave structure via the plasma potential [9–11]. If the added ion species is negatively ionized, then after a critical concentration of these negative ions, the plasma potential can even change its polarity to form a negative or rarefactive soliton [10, 11]. When an ion beam is injected into such a plasma, beam-plasma interaction makes the evolution even more complex in terms of nonlinear wave structures compared to a simple plasma [11–13]. For this reason, investigations on the plasmas with negative ions as one of the constituents has always been a topic of interest. Plasmas in astrophysical and space environments such as cometary tails, planetary ionospheres, and interstellar and molecular clouds usually are inherently multi-species with two or more than two types of ions and offer a rich platform for studying a variety of wave motions with subtle intricacies [14, 15]. These multi-species plasmas with negative ions are also easily produced in a laboratory and are well studied owing to their vital role in major scientific and technological applications such as plasma processing or fusion plasmas [8]. However, the response of a PINI plasma to an external charged debris is a topic yet to be explored fully. Moreover, as we explain in the next subsection, we raise a fundamental question about plasma-debris interaction – can other nonlinear processes mimic debris-induced nonlinearities? As we shall see, under certain circumstances, this is indeed true. So, we believe that an investigation of nonlinear wave propagation in a PINI plasma embedded with an external charged debris is definitely a topic worth studying, which should help us in understandings about the intricacies of the processes leading to formation of these nonlinear structures in multicomponent plasma.

Earlier and recent studies by several authors [16–19] on phenomena involving debris-induced nonlinearities identified the compressive structures in the precursor and wake regions of debris as well as pinned solitons at the location of the debris. This work shows that rarefactive structures can also be excited by debris, owing to the presence of negative

^a mpbora@gauhati.ac.in

ions. Notably, for the same debris velocity, the morphology of the excited waves in the three regions varies significantly with the concentration of negative ions. The new findings also show certain qualitative similarities with structures observed in other experimental processes suggesting a broader universality in the underlying nonlinear wave excitation mechanisms.

A. Can other processes mimic debris-induced nonlinearities?

Effect of presence of external debris in a flowing plasma has definitely gathered attention in recent years, especially as awareness and knowledge about interaction of space debris in low-earth orbits with ionospheric plasmas have come to the forefront of space research [16–23]. Though science of detection of space debris through debris-induced plasma interaction is still quite speculative, we are definitely learning more and more about it, as research intensifies in this area. In this context, we would like to raise a fundamental question about the similarities of the dynamics and structures of nonlinear waves in a plasma in general, to those induced by external charged debris. We do hope that we shall be able to clear some issues about this question through the present work.

In many experiments involving beam-plasma interactions, the beam is produced *in situ*, which leaves the plasma quasi-neutral. Different nonlinear structures produced due to these interactions have interesting dynamical signatures. In such cases, if the beam velocity v_b is $\ll v_s$ (v_s is the effective sound velocity), the propagating IAW does not *see* the Debye-scale disturbances created by the beam. This is analogous to what is known as ‘plasma approximation’, which requires $(k\lambda_D)^2 \ll 1$ to be applicable, where k is the wave number of the IAW and λ_D is the electron Debye shielding length. We argue that so long as v_b remains considerably smaller than v_s , the plasma quasi-neutrality is maintained. However as $v_b \sim v_s$, the beam-plasma dynamics start getting affected by the IAW. And when $v_b \gg v_s$, the situation becomes quite different and the beam dynamics will be completely *detached* from the ion-acoustic dynamics. If we now consider the ion-acoustic time scale τ_{IA} , it comes out to be $\sim 0.01 - 0.5$ millisecond for a typical laboratory device. On the other hand, the electron-ion collision time τ_{ei} is quite large ~ 5 millisecond for such parameters. As a result, when $v_b \gg v_s$, there is no way that thermalization can occur between the beam and the background plasma and the background plasma should *see* the beam as an external charged perturbation (debris) and the beam-plasma dynamics should closely mimic the dynamics observed in plasma-debris interaction. In subsequent sections, we show that this is indeed true and can be proven quite reasonably. We also see similarities among the nonlinear structures produced by externally induced perturbation in plasma to that of debris-induced perturbation. In this regard debris-induced perturbations can be thought to be quite commonplace in many experimental arrangements.

In this work, we explore different nonlinear structures excited by a moving charged debris in a multicomponent PINI plasma and also look at the similarities of their characteristics with different experimental results. The complete plasma system is modeled using a forced Korteweg–de Vries (fKdV) equation and results from theoretical analysis are verified using a 1-D multi-fluid flux-corrected transport simulation code (mFCT) [22]. The paper is organized as follows. The detailed plasma model and the governing equations are described in Section II. Section III contains the description of the fKdV dynamics and interpretation of its results. The results of Section III are verified using FCT simulation in Section IV. In Section V, we briefly address the variation of nonlinearity with debris velocity and in Section VI, we conclude.

II. PLASMA MODEL AND GOVERNING EQUATIONS

The model we are going to consider is a 1-D warm positive ion-negative ion (PINI) dissipation-less plasma with an external charge debris embedded into it. The relevant equations are the continuity and momentum equations for positive and negative ions. The equations are closed by the Poisson equation. The electrons are considered to be Boltzmannian. The equations are given by

$$\frac{\partial n_{\pm}}{\partial t} + \frac{\partial}{\partial x}(n_{\pm}v_{\pm}) = 0, \quad (1)$$

$$n_+ \frac{dv_+}{dt} = -\sigma \frac{\partial n_+}{\partial x} - n_+ \frac{\partial \phi}{\partial x}, \quad (2)$$

$$n_- \frac{dv_-}{dt} = -\frac{\sigma}{\mu} \frac{\partial n_-}{\partial x} + \frac{n_-}{\mu} \frac{\partial \phi}{\partial x}, \quad (3)$$

$$\frac{\partial^2 \phi}{\partial x^2} = n_e - \delta n_+ + (\delta - 1)n_- - \rho_{\text{ext}}, \quad (4)$$

where (n_{\pm}, v_{\pm}) are positive and negative ion densities and velocities respectively and ϕ is the plasma potential. The quantity $\sigma = T_i/T_e$ is the ratio of ion temperature to that of the electrons. Here, we have taken the temperatures

of positive and negative ions to be equal $T_i = T_+ = T_-$. The mass ratio of negative to positive ions is denoted by $\mu = m_-/m_+$ and $\delta = n_{+0}/n_{e0}$ is the ratio of the equilibrium positive ion density to the equilibrium electron density. In order to be able to compare our analytical results with existing laboratory experiments, we have assumed $m_+ > m_-$, which is mostly the case in case of experiments [10–13, 24]. In the above equations, the densities are normalized by their respective equilibrium values and potential is normalized by (T_e/e) with temperature expressed in energy unit. Time is normalized by ω_i^{-1} , with $\omega_i = \sqrt{n_{e0}e^2/(m_+\epsilon_0)} \equiv \delta^{-1/2}\omega_{p+} \equiv (\delta - 1)^{-1/2}\omega_{p-}$, where $\omega_{p\pm}$ are the respective positive ion and negative ion plasma frequencies. While length is normalized by electron Debye length, velocities are normalized by the ion sound speed $c_s = \sqrt{T_e/m_+}$, determined by the mass of the heaviest species. The quantity $\rho_{\text{ext}} \equiv \rho_{\text{ext}}(x - v_d t)$ is the normalized charge density of the external debris with v_d as the normalized velocity of the external debris. The overall charge neutrality of the PINI plasma without external debris is ensured through the relation

$$n_{e0} + n_{-0} = n_{+0}. \quad (5)$$

The normalized electron density is given by $n_e = e^\phi$.

An explanation about the ‘dissipation-less’ assumption is given in Section III (just before Section III-A), where it is more appropriate to discuss it with reference to the KdV equation.

A. The morphology of debris-induced nonlinearities

Before we investigate the nonlinear waves and structures induced by a charged debris in a PINI plasma, it is of relevance to discuss a bit about the fundamental physics of these nonlinearities in an $e-i$ plasma. We now know that the response of an $e-i$ plasma to an embedded charged debris very well depends on the nature of the charge of the debris [22]. It has been *only* recently shown that the formation of bright pinned solitons in the ion-acoustic regime due to the presence of negatively charged debris is basically a manifestation of the trapped ions in phase-space vortices formed due to ion-ion counter streaming instability (IICSI) [19]. Besides, proper spatial resolution of the pinned solitons requires a certain relative velocity between the debris and the plasma, though higher relative velocities may cause the pinned solitons to disappear [17, 19]. In contrast, a positively charged debris creates an ion hole, exciting an ion-acoustic wave (IAW), which propagates away from the site of the debris. However, when there is a relative motion between the debris and the plasma, the IAW becomes a dispersive shock wave (DSW) in the precursor region [22].

Following the above explanation, we expect that the response of a PINI plasma to external charged debris should also be characteristically different for positively and negatively charged debris. We further expect that for $\delta \sim 1$, the response should be similar to that in an $e-i$ plasma.

B. Mathematical reduction

We note that the above plasma model can be analyzed both mathematically and numerically. Typically, in these class of problems, one uses a scale transformation and reduces it to a pseudo potential (or Sagdeev potential) form [25] through the Poisson equation, which guarantees a soliton solution, though not necessarily a ‘sech’-type solution as one would have obtained through a KdV equation [26]. The other two approaches would be a reductive perturbation analysis to reduce the system to a KdV equation or a nonlinear Schrödinger equation (NLSE) [27]. However, with an external charged debris term, the model is simply not amenable to pseudo-potential analysis and that leaves us with other two options.

Employing the reductive perturbation method with the external charged debris term, we end up with either a forced-KdV (fKdV) or a forced-NLSE equation. At this point, we should emphasize that numerically we are going to use flux-corrected transport (FCT) method (as mentioned before) to simulate the dynamics, which is very efficient in detecting sharp discontinuities that can result from the debris-induced perturbation. Also the FCT formalism does not employ any approximations and solves the full set of equations, which in principle should provide us with both KdV-type as well as NLSE-type modulated wave solutions. However, the single hump perturbation that we expect from an external charged debris, the numerical solution is most likely to favor KdV-type solution which is also closer to the real-world and observable dynamics. In what follows, we shall therefore analyze the above model mathematically, using the fKdV equation only.

III. FORCED-KDV DYNAMICS

We shall now see, what forced-KdV (fKdV) dynamics has to offer. The fKdV equation is derived using the usual reductive perturbation theory by using the following expansions, assuming a static and neutral equilibrium. The external charged debris is introduced as a second order perturbation. The expansions are

$$n_{\pm} \simeq 1 + \varepsilon n_{\pm}^{(1)} + \varepsilon^2 n_{\pm}^{(2)} + \dots, \quad (6)$$

$$v_{\pm} \simeq \varepsilon v_{\pm}^{(1)} + \varepsilon^2 v_{\pm}^{(2)} + \dots, \quad (7)$$

$$\phi \simeq \varepsilon \phi^{(1)} + \varepsilon^2 \phi^{(2)} + \dots, \quad (8)$$

$$\rho_{\text{ext}} = \varepsilon^2 \rho_{\text{ext}}^{(2)}, \quad (9)$$

where ε is the expansion parameter, which is $\ll 1$. One question related to the order of perturbation for the external charged debris may naturally arise here. In this context, two points to be noted here – that we use the KdV equation for weak nonlinearity only and how strong a perturbation an external charged debris may induce in the bulk plasma. Our assumption of using a second order perturbation for the debris is quite in line with the weak nonlinearity assumption on the basis of which the KdV equation is derived. As far as the strength of perturbation is concerned, we shall see in subsequent sections that the experimentally observed nonlinearities are quite close to our numerical solutions (obtained via FCT simulation) as well as the fKdV solutions, which demonstrates that our assumption of introducing the external charged debris as second order perturbation is indeed consistent. Besides, using a second order perturbation for debris leaves us with the simplest form of fKdV equation.

We now use the stretched variables $\xi = \varepsilon^{1/2}(x - Vt)$ and $\tau = \varepsilon^{3/2}t$ for space and time coordinates, where V is the dimensionless phase velocity of the IAW. Following the usual procedure, by collecting the first order terms, we have the following expressions for the first order variables in terms of $\phi^{(1)}$,

$$n_+^{(1)} = \frac{\phi^{(1)}}{V^2 - \sigma}, \quad (10)$$

$$n_-^{(1)} = -\frac{\phi^{(1)}}{V^2 \mu - \sigma}, \quad (11)$$

$$v_{\pm}^{(1)} = V n_{\pm}^{(1)}, \quad (12)$$

where the phase velocity expression (or the compatibility condition) is given by

$$V = \left[\frac{\alpha + \sqrt{\alpha^2 - 4\mu\sigma(2\delta + \sigma - 1)}}{2\mu} \right]^{1/2}, \quad (13)$$

with $\alpha = (\mu + 1)(\delta + \sigma) - 1$. Collecting the next higher order terms and eliminating the second order quantities, using the Poisson equation, we finally get the fKdV equation as follows

$$\partial_{\tau} \phi^{(1)} + A \phi^{(1)} \partial_{\xi} \phi^{(1)} + B \partial_{\xi}^3 \phi^{(1)} = -B \partial_{\xi} \rho_{\text{ext}}^{(2)}, \quad (14)$$

where nonlinear and dispersion coefficients A and B are given by

$$A = \left[\frac{(b + 2V^2)\delta}{b^3} - \frac{2(\delta - 1)V^2\mu}{a^3} - \frac{(\delta - 1)}{a^2} - 1 \right] B, \quad (15)$$

$$B = \left[2V \left\{ \frac{(\delta - 1)\mu}{a^2} + \frac{\delta}{b^2} \right\} \right]^{-1}, \quad (16)$$

and $a = (V^2\mu - \sigma)$ and $b = (V^2 - \sigma)$.

We note that unlike the KdV equation, the fKdV equation, in general, is non-integrable and has to be solved numerically. So, we present the numerical solutions of Eq.(14) for a Gaussian charge density profile for the external debris with periodic boundary conditions. Here, we consider two possible scenarios – positively charged debris (Section III-A) and negatively charged debris (Section III-B). For positively charged debris, we also compare the debris-induced nonlinearity with results from two different experiments, both of which employ different mechanisms to excite nonlinear waves. All the figures in the subsequent sections are drawn in the rest frame of the debris. We present our results with respect to two independent parameters – δ and v_d for a fixed σ .

As mentioned before, we now provide an explanation about our ‘dissipation-less’ assumption of the plasma model. The dissipation in this case may come in two flavors – through collisions and Landau damping. There are examples of work involving multicomponent plasma (not necessarily PINI plasma) with collisions as well as with Landau damping term [28]. While the inclusion of different collisional terms in the fluid model is quite straight forward [29, 30], the same is not true in the case of Landau damping. However, as shown by VanDam [31], it is indeed possible to include a dissipation-like term arising out of wave-particle resonance (Landau damping) in a KdV-like formalism. In Section III-A.1, while comparing our fKdV solutions with ion-beam-induced nonlinearities, we shall see that the e - i collision time $\tau_{ei} \sim 3.5$ millisecond. However, the ion-acoustic time scale, which is the characteristic time scale of this work, is $\tau_{IA} \sim 0.03$ millisecond. So, we can probably safely neglect collisional dissipation. Coming back to now Landau damping, VanDam [31] has shown that a dissipation-like term can be incorporated into the KdV equation with the linear Landau damping rate $\gamma = \tilde{\gamma}|k|$ (see Appendix A) where

$$\tilde{\gamma} = \frac{\lambda}{\alpha \varepsilon \sqrt{2\pi}} \left[\left(\frac{m_e}{m_+} \right)^{1/2} + \sigma^{-3/2} \exp \left(-\frac{\lambda^2}{2\sigma} \right) \right], \quad (17)$$

with

$$\lambda = 1 + \frac{3}{2}\sigma, \quad (18)$$

$$\alpha = 2\lambda^{-2} - 3\lambda^{-4}\sigma. \quad (19)$$

In the above expression, k is the wavenumber of the associated IAW. The expansion parameter can be taken as $\varepsilon \sim \sigma^{-3/2}e^{-1/(2\sigma)}$ [31]. This expression is written with the assumption that the momentum of the resultant IAW in a PINI plasma is carried primarily by the heavier positive ions. With typical parameters used in this work (see Section III-A.1), we find that the damping timescale τ_γ corresponding to γ is ~ 1 millisecond, which is more than two orders of magnitude larger than τ_{IA} . So, owing to the fact that $\tau_\gamma \gg \tau_{IA}$, we can safely neglect the effect of Landau damping in this work.

A. Positively charged external debris

The first set of results shown in Fig.1 are for debris with a positive charge $\rho_{\text{ext}} > 0$ at the end of $\tau = 100$ with $\sigma = 0.1$. The figure shows the nonlinear waves in $\phi \equiv \phi^{(1)}(\xi, \tau)$. The charge density distribution of the debris is a Gaussian-shaped distribution (see below) $\rho_{\text{ext}}(\xi) = \rho_0 e^{-\xi^2/\Delta}$, where ρ_0 is the peak of the distribution and width is determined by Δ [16]. We note that the external debris is introduced as a perturbation with ρ_0 denoting the strength. In all the cases (unless indicated otherwise), we have used a perturbation with $\rho_0 = 0.5$ which is equivalent to a perturbation $\equiv 50\%$ of the equilibrium density. In the figure, the shaded region shows the extent of the debris charge distribution centered in the middle of the frame indicated by the dashed vertical line. The debris move with a velocity v_d from right to left. In Fig.1(a), we observe that for low (subsonic) v_d , the debris excites bright ion-acoustic solitons which move away from the debris in the precursor region. We also observe that the velocities of these solitons increase from being subsonic to becoming supersonic as δ increases from 1.02 to 1.8. The changing shape of the soliton for increasing δ can be attributed to the increasing negative ion density (with higher δ) which tend to accelerate from left to right as a response to the positive perturbation at the debris site. We further note that in the production of a PINI plasma, experimentalists usually use an electronegative gas in an e - i plasma to create negative ions at the expense of less warm electrons. So, an increase of δ causes an increase in negative ion density in a PINI plasma and the increase of velocity of the soliton can be attributed to the increase in negative ion density. However, as debris velocity increases and becomes sonic, higher δ perturbations slow down in comparison to lower δ perturbations which ultimately forms dark pinned solitons as debris velocity increases more, as shown in the three panels on the right in the figure, Fig.1(d), (e), and (f). As v_d increases, pinned solitons tend to form at the debris position for higher δ whereas low δ perturbations never get to form pinned solitons and remain predominantly a positive nonlinearity in the form of a DSW in the precursor region. The assumption of Gaussian-shaped distribution for the charge density of a debris of size $\gg \lambda_D$ can be fairly ascertained, if the parameter $\beta_e \ll 1$ (for negatively charged debris), with

$$\beta_e = \frac{e^2}{4\pi\epsilon_0 R T_e}, \quad (20)$$

where e is the electronic charge and R is the radius of a spherical debris [32]. This result is rigorously proved for impurity particles in a plasma using the orbit motion limited (OML) theory [33] and numerical simulation, which can be readily interpreted for charged debris as well. This can also be extended to debris with positive charge.

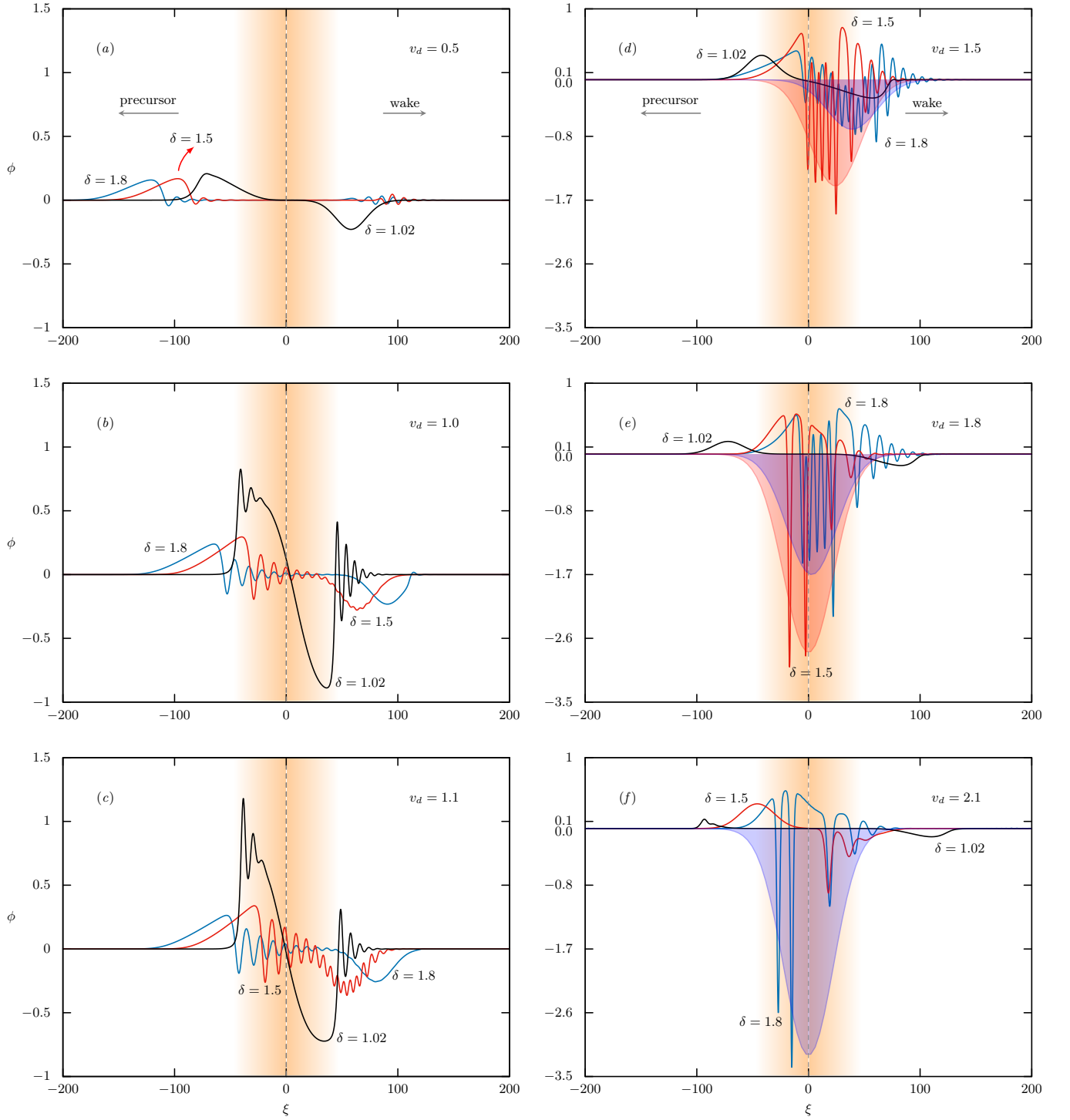


Figure 1. Nonlinear wave for a flowing PINI plasma with a positively charged external debris. All panels are drawn in the rest frame of the debris, which is in the middle of a panel, denoted by a vertical dashed line. The shaded vertical regions indicate the extent of the charged debris. The shaded envelopes on the right hand panels indicated the envelopes of the corresponding dark pinned solitons.

If we now consider the case of charged debris in space plasma in low earth orbit (LEO), the size of the debris can vary from being very small to very large, but anything larger than a few Debye length is capable of inducing nonlinear structures. Considering typical parameters for LEO plasma [34, 35], the value for β_e comes out to be $\sim 10^{-6}$ even for $R \sim \lambda_D$. For ions (positively charged debris), this comes out to be $\beta_i \sim 10^{-3}$. In laboratory experiments involving debris $\beta_e \sim 10^{-5}$ assuming debris of size $\sim \lambda_D$ [36].

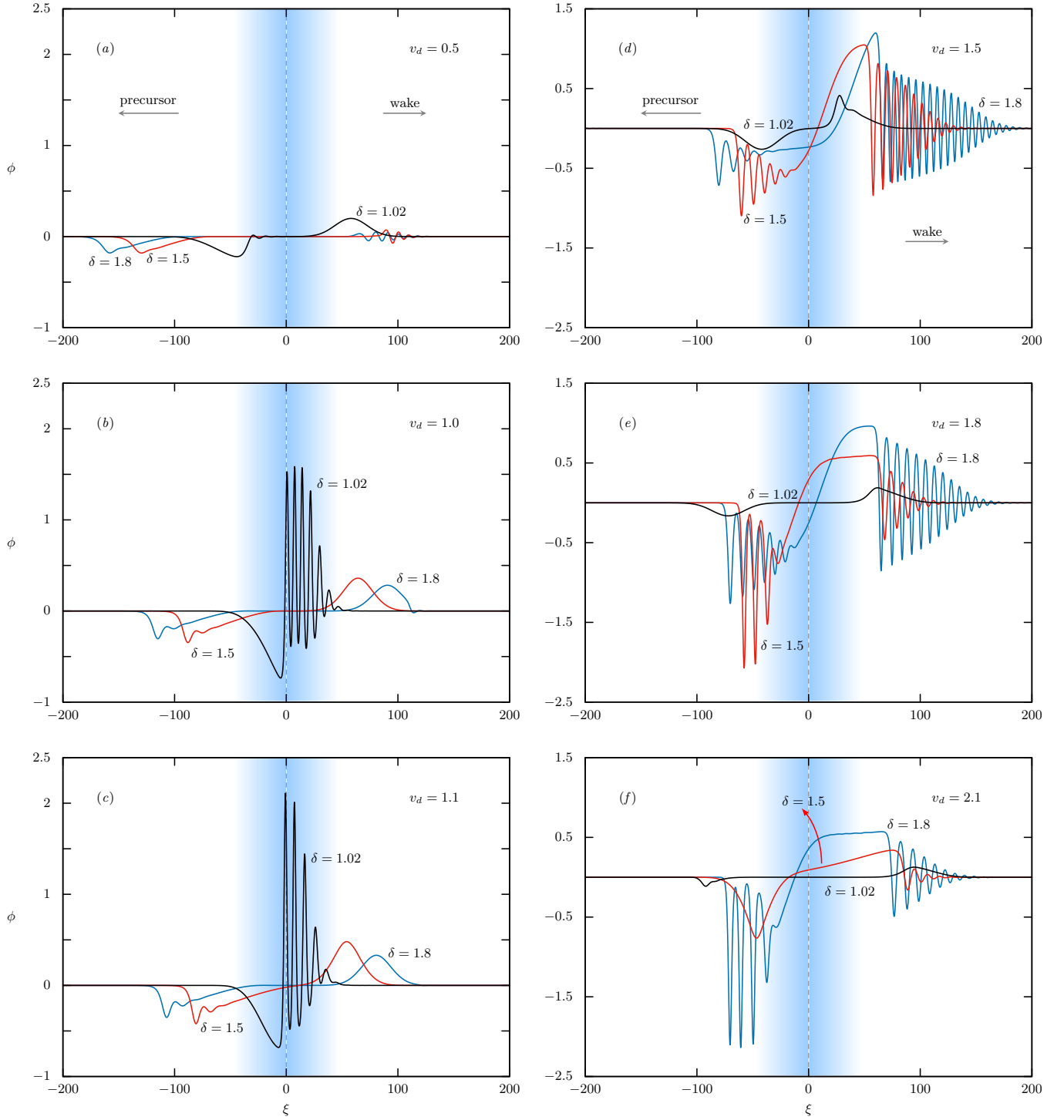


Figure 2. Nonlinear wave for a flowing plasma with a negatively charged external debris. All other particulars are same as in Fig.1. The shaded vertical regions indicate the extent of the negatively charged debris.

These results are entirely in conformity with what we know about formation of debris-induced pinned solitons and DSWs. We now know that in an $e-i$ plasma the pinned solitons formed due to moving negatively charged debris is basically a manifestation of the ions trapped in the phase space vortices formed by the IICSI [19], whereas a positively charged debris induces a DSW in the precursor region. So, for $\delta \sim 1$ (very less concentration of negative ions), the plasma behaves like the usual $e-i$ plasma and no pinned solitons can form for a moving positively charged debris. However for $\delta > 1$, the negative ions are attracted by the positively charged debris causing a IICSI-like phenomena for

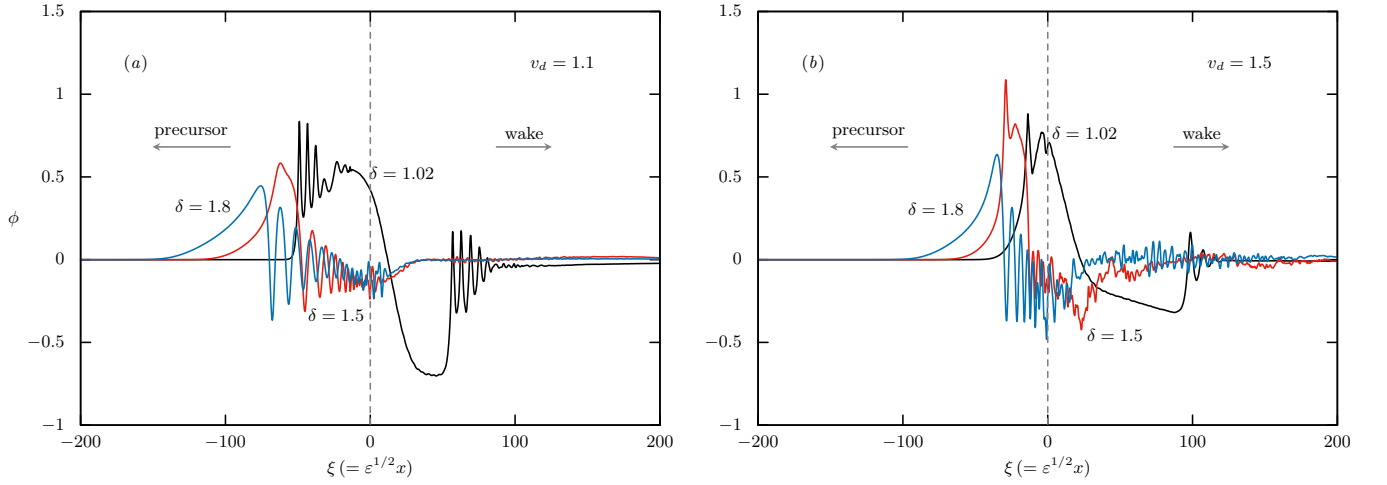


Figure 3. FCT simulation results of propagation of nonlinear wave in a PINI plasma with and embedded external positively charged debris. These results are equivalent to the theoretical cases obtained through fKdV solution shown in Fig.1. The left panel (a) in the above figure corresponds to Fig.1(c) and the right panel (b) above corresponds to Fig.1(d). These results are plotted at the end of $\tau = 100 \equiv \varepsilon^{3/2}t$.

negative ions, leading to the formation of phase space vortices which in turn cause formation of dark pinned solitons at the debris position.

1. Comparison with ion-beam-induced nonlinearities

Let us now discuss the first case where under certain circumstances, a positive ion-beam in a PINI plasma mimics the responses of a debris-induced nonlinearities. In this experiment, the positive ion-beam is produced in situ by accelerating a part of the ion population in the plasma so that overall quasi-neutrality is maintained throughout [11]. This case is also interesting as there are several investigations being carried out by different authors to analyze the formation of nonlinear structures in such plasmas [12, 13].

Let us consider such a three-component PINI plasma, consisting of positive ion (n_+), negative ion (n_-), and electron (n_e), in the presence of a positive ion beam (b^+), as considered in the experimental work by Nakamura [11] (N99 hereafter). Note that the whole system is to be considered quasi-neutral,

$$n_+ + n_{b+} = n_- + n_e = n_T, \quad (21)$$

which essentially requires that the positive ion beam to be created in situ. As a result, the formation of the positive ion beam causes an overall depletion of the bulk positive ions. The comparative concentration of negative ion is denoted by the quantity $r = n_-/n_T$, which can be written in terms of δ

$$\delta = \frac{1}{1-r}. \quad (22)$$

Let us now consider the slowest possible ion-acoustic time scale which is given by

$$\tau_{IA} = f^{-1} = \left[\frac{k}{2\pi} \sqrt{\frac{T_e}{m_+}} \right]^{-1}, \quad (23)$$

where $k = 2\pi/\lambda$ with λ being the wavelength of the ion-acoustic wave. In the above expression, T_e is the electron temperature which is ~ 1 eV and m_+ is the mass of the heaviest ion, which is Ar^+ , so that $m_+ \sim 40m_p$, where m_p is the mass of a proton. Assuming the experimental double-plasma device to be of length ~ 90 cm [11], we can assume the largest possible ion-acoustic wavelength to be ~ 0.45 m. With these parameters, we have $\tau_{IA} \sim 0.03$ milli second. If we now consider the electron-ion collision time τ_{ei} , we have

$$\tau_{ei} = \frac{6\sqrt{2}\pi^{3/2}\epsilon_0^2 m_e^{1/2} T_e^{3/2}}{n_e e^4 \ln \Lambda}, \quad (24)$$

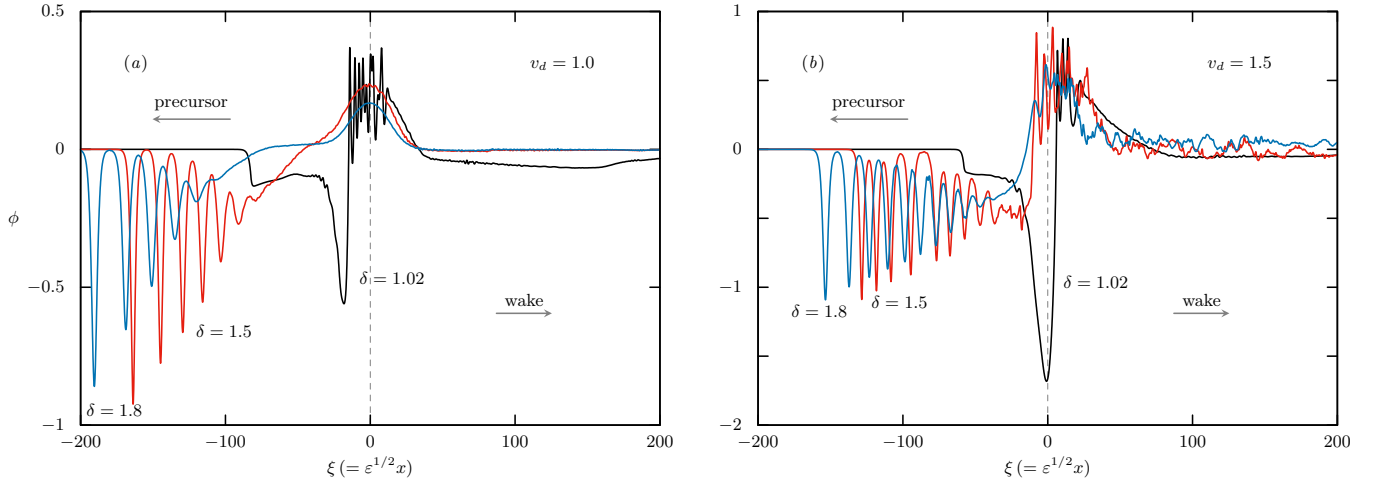


Figure 4. FCT simulation results of propagation of nonlinear wave in a PINI plasma with and embedded external negatively charged debris. These results are equivalent to the theoretical cases obtained through fKdV solution shown in Fig.2. The left panel (a) in the above figure corresponds to Fig.2(b) and the right panel (b) above corresponds to Fig.2(d). These results are plotted at the end of $\tau = 100 \equiv \varepsilon^{3/2}t$.

where $\ln \Lambda$ is the Coulomb logarithm $\sim 10 - 12$. For $n_e \sim 10^7 \text{ cm}^{-3}$ [11], we have $\tau_{ei} \sim 3.5$ milli second. We now argue that as $\tau_{ei} \gg \tau_{IA}$, it can be safely assumed that in the ion-acoustic timescale, the plasma will not be able to thermalize. As a result, a positive ion beam propagating through the plasma will not be able to thermalize with the bulk plasma and for all practical purposes, the beam will behave as an external debris. It has been observed in N99 that below a certain critical value for beam velocity, increasing r (higher δ) causes the nonlinearity to become negative from positive. However, beyond the critical value of the beam velocity, the nonlinearity remains positive irrespective of the initial pulse (which is reported only at higher δ in N99). In our case with debris as well, we see a similar behavior as evident from the panels in the left column of the figure i.e. Fig.1(a), (b), and (c). We can see that when debris velocity is $\lesssim 1.1$, for low δ (~ 1), there is a steepening in the leading edge indicating positive nonlinearity while for higher δ , the steepening is on the falling edge, which indicates negative nonlinearity. We note that the ‘positive nonlinearity’ in the case of a compressive or bright soliton is referred with respect to the nonlinear term $A\phi^{(1)}\partial_\xi\phi^{(1)}$ [see Eq.(14)] in a usual KdV equation (without the debris term), which is responsible for steepening of the leading edge of a soliton. On the other hand, when the steepening occurs in the falling edge, it is usually termed as ‘negative nonlinearity’. When debris velocity increases [Fig.1(f)], the negative nonlinearity which was observed for say $\delta = 1.5$ and with low v_d , decreases and get balanced by dispersion giving rise to a bright KdV soliton. These results are also confirmed through our FCT simulation, which are being presented in Section IV.

We should however be cautious not to compare the entire experimental results of N99 with the results obtained in this work, as the external charged debris in this work is a localized charged perturbation with no assumption of quasi-neutrality, while in N99 and other similar experimental works, the beam is an extended structure with definitive wake region. So, we can probably compare only the leading edge dynamics of a beam-plasma interaction with the precursor region of debris-induced nonlinearity.

2. Comparison with pulse-induced nonlinearities

Let us now consider a very recent experimental observation of large-amplitude perturbation in a PINI plasma by Pathak and Bailung [24] (P25 thereafter), where a positive pulse is induced externally to a PINI plasma resulting in a large-amplitude positive perturbation (up to 70% of equilibrium plasma density), which is then used to study the effect of controlled Landau damping on nonlinear IAW. This produces a dissipative shock front when dissipation (through Landau damping) becomes large.

We argue that dynamically, an external perturbation can be considered to be having the same effect as an external charged debris so far as the leading edge (or precursor region) is concerned. So, we can expect a similar behavior of nonlinear wave front for this external perturbation and perturbation induced by an external debris. In this context, we would like to compare our results as shown in the cases for $\delta = 1.02$ with $v_d = 1.0, 1.1$ in Fig.1(b) and (c) in the precursor regions and the case shown in Fig.4 of P25, which is comparable to our theoretical situation. In both cases,

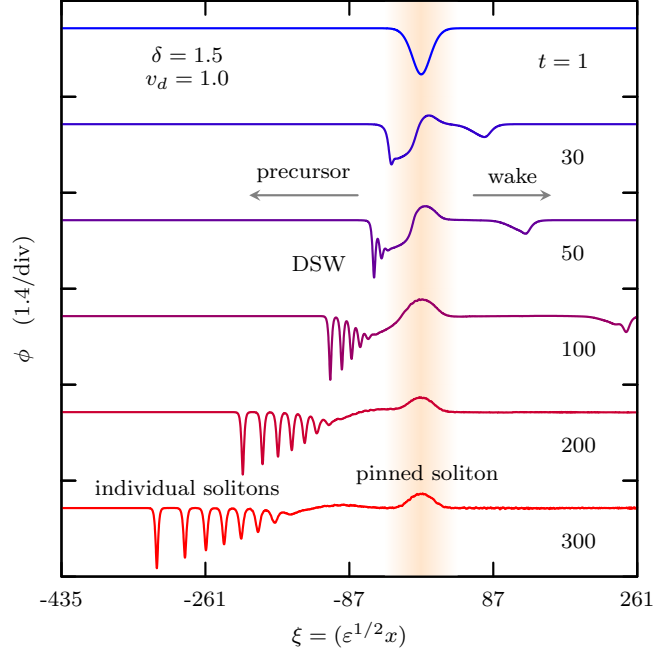


Figure 5. FCT simulation results showing evolution of a DSW in the precursor region over time for a negatively charged debris perturbation. Shaded region corresponds to the perturbation site.

we have a leading shock front with oscillations which are nothing but DSWs when there is no dissipation. Note that Fig.4 of P25 is for the case when Landau damping is negligible with negligible negative ions ($\delta \sim 1.0$). The situation is however different in the wake region (or trailing region of the pulse). This is due to the fact that experimentally a one-time external perturbation is induced by pushing a signal which then propagates in the form of discontinuity (either as a single soliton as a ramp structure) through the plasma which then transforms into a DSW as it moves. For the case of external debris however, the perturbation remains intact all throughout the life cycle of the nonlinear wave front giving rise to a very definitive signature in the wake region.

B. Negatively charged external debris

We now present the results for a negatively charged debris in a flowing PINI plasma in Fig.2. All the parameters are kept same as in the case for positively charged debris. The shaded regions in all the panels show the extent of the charged debris with the centered dashed line indicating the debris position. As expected, bright pinned solitons are formed for δ close to unity at $\delta = 1.02$, when the relative velocity between debris and PINI plasma v_d exceeds a certain value as shown in Fig.2(a) and (b). It can be clearly seen that as v_d increases, these pinned solitons finally vanishes even for $\delta \rightarrow 1$, which is consistent with our observations about pinned solitons in an $e-i$ plasma [17, 19]. For higher values of δ , IAWs in the precursor region propagate showing an oscillatory shock excitation which is not fully formed at a lower debris velocity. However as v_d increases, amplitude of the precursor wave-front also increases and fully developed DSWs are observed to be formed. Here, it is worth mentioning that, similar behavior was also reported for the propagation of a rarefactive pulse in presence of positive ion beam in high negative ion density plasma [13]. Increasing the beam velocity resulted in a rise in soliton amplitude and a knee formation at the downstream, culminating in the formation of a shock-like structure. A realistic fluid simulation for much longer time period shows that these DSWs, as they propagate away from the site of the debris, get transformed into a train of *individual* solitons after segregation of the peaks, about which we shall discuss in Section IV. The pinned solitons at the site of the debris are deformed due to the presence of the shock. Also, behind the debris, soliton-like structures are seen to be excited due to ion-acoustic oscillations.

IV. FLUX-CORRECTED TRANSPORT (FCT) SIMULATION

To corroborate the theoretical analysis presented in Section III, we now present an FCT simulation of the PINI plasma with an embedded external charged debris. We use a 1-D multi-fluid FCT code (*mFCT*) [22] based on Boris's original algorithm [37] with Zalesak's flux limiter [38]. The FCT formalism requires the hydrodynamic equations Eq.(1-3) to be put in the form of a generalized continuity equation,

$$\frac{\partial f}{\partial t} = -\frac{\partial}{\partial x}(fv) + \frac{\partial s}{\partial x}, \quad (25)$$

where $f = (n_+, n_-, n_+v_+, n_-v_-)$ is the physical quantity to be solved, (fv) is the corresponding flux, and s is the source term. The external charged debris is entered through the Poisson equation Eq.(4) as before which is to be solved at every time step along with Eq.(25). We must however emphasize that the FCT simulation results contain both KdV-type and NLSE-type nonlinear solutions with the latter being less dominant. Nevertheless, in certain parameter regimes, we might see a considerable deviation of the simulation results from fKdV solutions.

Our FCT simulation results are presented through Fig.3 for the case with positively charged debris and through Fig.4 for negatively charged debris. In Fig.3, we have shown the results of the FCT simulation for the fKdV cases shown in Fig.1(c), corresponding to Fig.3(a) and Fig.1(d), corresponding to Fig.3(b). These curves are plotted at the end of $\tau = 100 \equiv \varepsilon^{3/2}t$. The x -axis is also respectively scaled for $\xi \equiv \varepsilon^{1/2}x$. Our estimate shows that the effective $\varepsilon \sim 0.7$ for $\rho_0 = 0.5$, which is used in the fKdV solution as well as in the FCT simulation. In both cases, the external charged debris is a Gaussian profile given by $\rho_{\text{ext}}(\xi) = \rho_0 e^{-\xi^2/\Delta}$. As we can see that the simulations results are quite comparable to those obtained from the corresponding fKdV solutions, except in the case for $\delta = 1.5$ and $v_d = 1.5$, which can be attributed to slightly different time over which various nonlinearities develop in a simulation and in fKdV solutions.

We now present the simulation results for negatively charged debris in Fig.4. All other parameters except the debris charge is same as in the case of Fig.3. Fig.4(a) corresponds to the fKdV solution presented in Fig.2(b) ($v_d = 1.0$) and Fig.4(b) corresponds to Fig.2(d) ($v_d = 1.5$). We observe that bright pinned solitons for $\delta = 1.02$ and DSWs for higher δ are properly captured in the FCT simulation, while the DSWs seem to be fully formed in the fKdV solutions only when $v_d = 1.5$. Besides, the distinct soliton-like structures in the wake regions of the fKdV solutions for both $v_d = 1.0$ and 1.5 seem to be absent in the simulation. Instead, singly peaked pinned solitons with almost no wakes for $v_d = 1.0$ and peak-modulated pinned solitons [17] and a turbulent wake trail due to the propagating shock for $v_d = 1.5$ are found to exist. These discrepancies between the fKdV solution and FCT simulations perhaps can be attributed to the weak nonlinearity approximation that is in-built in the fKdV derivation, while in FCT simulation there is no approximation on nonlinearities involved. As a result, nonlinear oscillations and structures tend to be more prominent in the simulation, which might also contain modulated wave-packet-like solutions (forced NLSE type). Nevertheless, we believe that to large extent the fKdV dynamics is similar to the FCT simulations and our observations about similarities between debris-induced nonlinearities and nonlinearities introduced by positive ion-beam and large-amplitude perturbation in a PINI plasma can be fairly ascertained.

It is important to note that the DSWs seen in Fig.2 and 4 are called ‘quasi-steady state shocks’ [39] as the initial oscillatory shock profile is not retained over a longer time period ($t \geq 200$). Fig.5 shows the potential distribution of one such shock profile at different time-steps ($t = 0 - 100$). Initially, the external charge perturbation introduces a highly nonlinear IAW and the leading edge of the precursor becomes steepened which forms a DSW with an oscillatory tail behind due to its dispersive nature. This non-steady shock profile, after a relatively long time ($t \geq 200$), transforms into a train of individual propagating solitons as nonlinearity gets balanced by dispersion and each and every oscillatory peaks in the DSW separates into individual soliton structures. This effect is already observed and confirmed by earlier investigations on ion-acoustic shock waves both in theory and experiments [39]. The positive hump observed at the site of the debris is the signature formation of a single-peak bright pinned soliton.

V. DEBRIS VELOCITY AND NONLINEARITY

One very interesting phenomenon is the changing property of the nonlinearity with increasing debris velocity which is similar to what is observed experimentally with respect to beam velocity in a PINI plasma [12]. From our analysis, what we observe is that as debris velocity increases, the wave amplitude steadily increases until reaching a maximum and then decreases, which is seen from the steepening in the leading edge (precursor region), which then gradually changes to a DSW before becoming a train of solitons and then a single KdV-like soliton. While the steepening in the leading edge indicates a dominant positive nonlinearity over dispersion at low debris velocity, as debris velocity increases, nonlinearity decreases and gets balanced by dispersion which creates a KdV-like soliton.

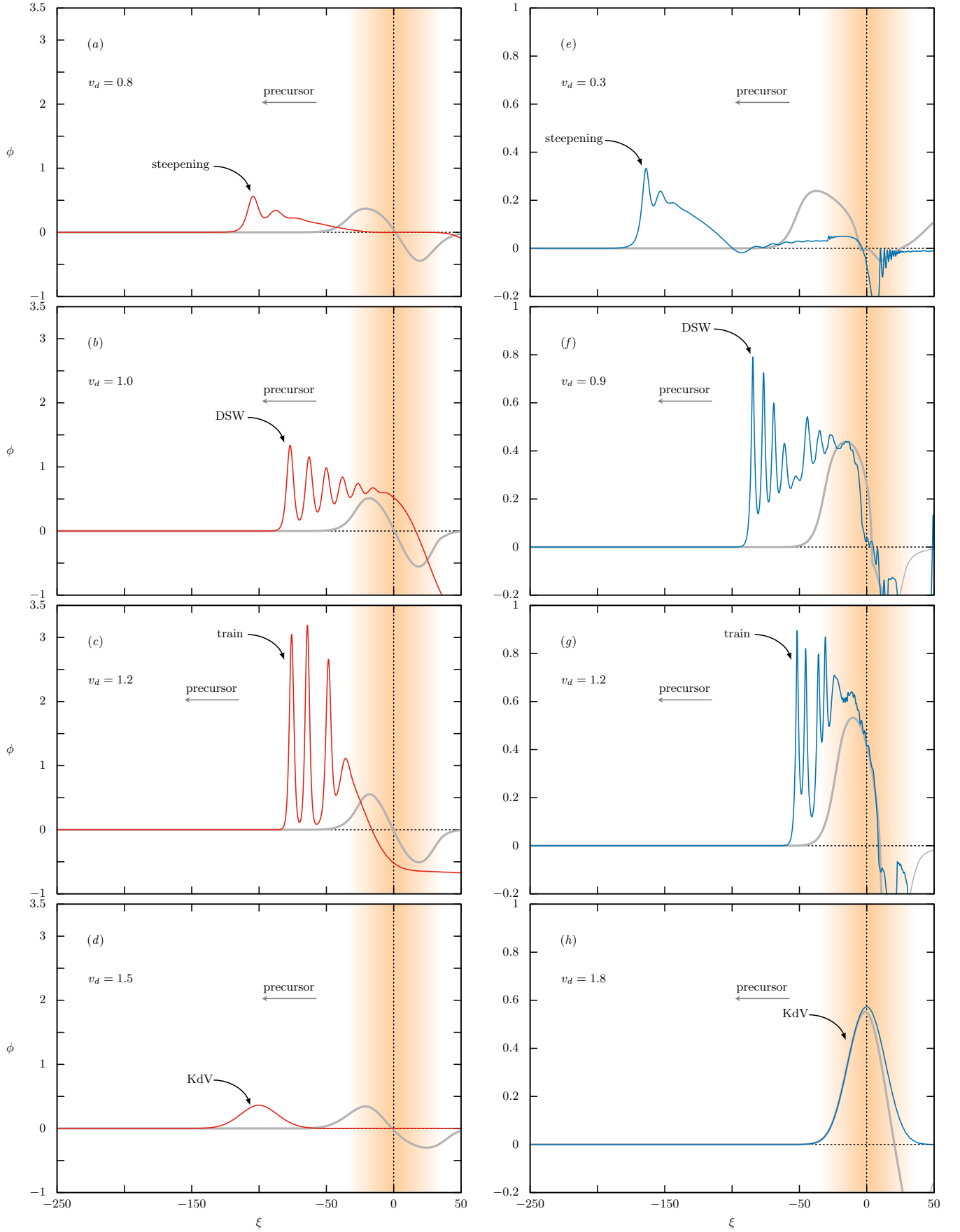


Figure 6. The changing nonlinearity with increasing debris velocity (from top to bottom) as obtained from the fKdV solutions (left column) and FCT simulation (right column). The thick, gray pulse in each frame is the debris-induced perturbation at the initial stage of the evolution which has later transformed into their respective form as time progresses.

In Fig.6, we show this effect as obtained from the fKdV solution [left column Fig.6(a-d)] and from FCT hydrodynamic simulation [right column Fig.6(e-h)]. In this figure, we have indicated the changing nonlinearity with an arrow with the keywords ‘steepening’, ‘DSW’, ‘train’, and ‘KdV’, respectively to indicate the phenomenon of steepening in the leading edge, formation of DSW, transformation to a train of solitons, and finally a simple KdV soliton as debris velocity v_d increases from 0.8 to 1.5 for fKdV solutions and from 0.3 to 1.8 for FCT solutions. All the panels in the above figure are drawn at the rest frame of the debris, which is moving toward left. The thick, gray colored pulse in each frame indicates the initial stage of the perturbation induced by the moving debris which has later transformed. Density ratio (δ) and ion to electron temperature ratio (σ) are taken to be 1.05 and 0.05 respectively, in both cases. It is important to note that all these evolutions are drawn at the same time evolution (column wise) across different v_d . The parameters are slightly different for fKdV and FCT solutions which are optimized respectively to represent this effect. This parameter difference of fKdV and FCT solutions can be attributed to the weak nonlinearity approximation that is inherent in the KdV formalism and full hydrodynamic simulation through FCT simulation.

We should also note that all these nonlinearities change their behaviors as the plasma evolves in time. For example, a steepening of the leading edge will eventually transform itself into another form as we evolve the system in time. This is also evident from the similar experimental observations [12, 13]. In this context we would like to recall that a pure KdV equation is integrable with ‘sech’ solution which *does not* get evolved in time. However, an fKdV equation is inherently non-integrable and different nonlinear solutions of the fKdV equation such as DSW or pinned solitons are necessarily transient phenomena and are bound to evolve in time. As per the parameters used in the FCT simulation, assuming an equilibrium plasma number density of $\sim 10^6 \text{ cm}^{-3}$, the entire spatial nonlinear evolution frame shown in Fig.6 is contained within $\sim 25 \text{ cm}$, which is quite comparable to distance over which these phenomena are observed in contemporary plasma devices [12, 13].

VI. SUMMARY AND CONCLUSION

To summarize, we have presented a detailed study of external debris-induced nonlinear structures in a multicomponent positive ion-negative ion (PINI) plasma. The motivation to choose a PINI plasma for this study is primarily due the fact that PINI plasmas are easily produced in low-temperature laboratory devices and also are widely used in plasma processing experiments. Additionally, theoretical and experimental (laboratory and also space-based) studies of debris-induced nonlinear plasma phenomena have been recently generating a lot of interests among the plasma physicists, especially due to the renewed attention of the scientific community in detection and removal of space-debris from low-earth orbits. Besides a detailed analysis of nonlinear waves excited by external charged debris, we also point out the similarities in certain characteristics with those excited by a high velocity positive ion beam and large amplitude pulse perturbations in such plasmas. The important findings of our analysis are presented below.

Debris-induced nonlinear waves

- For positively charged debris moving with subsonic velocities, small amplitude bright solitons are observed with steepening in the leading edge in low δ (low negative ion density) plasmas. On the other hand, steepening starts on the falling edge of the wave as δ is increased beyond certain value and as debris velocity reaches sonic and supersonic regime, large amplitude dark pinned solitons are excited. However, for the same velocity regime, DSWs are seen to be formed in low δ plasma. At very high debris velocity, the precursor wave is found to transform into a KdV like soliton.
- On the contrary, for perturbation induced by a negatively charged debris, the nature and morphology of nonlinear structures are exactly opposite to what is observed in the case of positively charged debris. Presence of higher concentration of negative ion species (high δ) leads to formation of quasi-static DSWs as debris velocity becomes supersonic and bright pinned solitons are formed in the presence of lower concentration of negative ions (low δ). However, the nature of nonlinearity of the excited waves remains the same as in the case of a positive debris perturbation.
- Toward the end, we have also shown how the KdV nonlinearity gets modified by the nonlinearity introduced by the external debris as debris velocity increases. This observation also has the similarity with the phenomenon of changing property of the nonlinear wave resulting out of beam-plasma interaction as beam velocity increases [11–13].

Can other processes mimic debris-induced nonlinearity?

We have argued that a high velocity ion beam would behave analogous to an moving external charge debris as long as the ion-acoustic timescale is smaller than the electron-ion collision time ($\tau_{IA} \ll \tau_{ei}$) or beam ions move faster without remaining in phase with plasma waves, thus hindering beam plasma energy transfer process and would affect nonlinear wave dynamics via the electric field, similar to an external charge perturbation.

- Toward this, we observe a resemblance between the DSWs excited by a moving debris in a low negative ion density PINI plasma to the oscillatory IA shocks excited by positive ramp signal in absence of the negative ions [24].
- Similarly, DSWs are observed to be excited by negatively charged debris in a high δ plasma when debris velocity crosses the sound speed which are also observed in negative pulse-excited high negative ion density plasma with a positive ion beam [13].
- We have also observed that positively charged debris introduce a positive nonlinearity when the negative ion concentration is low (low δ), while the same debris excites a negative nonlinearity when the negative ion concentration is high (high δ). This phenomenon is similar to what is observed with a positive ion beam in a PINI plasma [11].
- Further the amplitudes of nonlinear waves are observed to increase for both positive and negative perturbation with increase in the debris velocity, which is similar to the case of increasing beam velocity in PINI plasma [11–13].

This work advances the understanding of externally driven nonlinear wave dynamics in multicomponent plasmas, offering a broader perspective on the applicability and limitations of perturbative approaches. The observed similarities between debris-driven nonlinear structures and those due to other processes provide insights into the underlying mechanisms and may help in the interpretation of future experimental results involving negative ion plasmas.

ACKNOWLEDGMENTS

The authors would like to thank Kalpana Bora for critical reading of the revised manuscript and the anonymous referees for their suggestions. One of the authors, HS thanks CSIR-HRDG, New Delhi, India for Senior Research Fellowship (SRF) research grant 09/059(0074)/2021-EMR-I.

APPENDIX A

In this Appendix, we try to estimate the Landau damping rate for a simplified electron-heavy ion plasma where we have neglected the negative ion species. For this case, using a reductive perturbation theory along with the kinetic correction due to linear Landau damping of the IAW, we have a KdV-like equation [31]

$$\partial_\tau \phi^{(1)} + \frac{\beta}{\alpha} \phi^{(1)} \partial_\xi \phi^{(1)} + \frac{1}{\alpha} \partial_\xi^3 \phi^{(1)} + \tilde{\gamma} \cdot \mathcal{P} \int_{-\infty}^{+\infty} \frac{\partial \phi^{(1)}}{\partial \xi'} \frac{d\xi'}{\xi - \xi'} = 0, \quad (\text{A1})$$

where

$$\lambda = 1 + \frac{3}{2}\sigma, \quad (\text{A2})$$

$$\alpha = 2\lambda^{-2} - 3\lambda^{-4}\sigma, \quad (\text{A3})$$

$$\tilde{\gamma} = \frac{\lambda}{\alpha \varepsilon \sqrt{2\pi}} \left[\left(\frac{m_e}{m_+} \right)^{1/2} + \sigma^{-3/2} \exp\left(-\frac{\lambda^2}{2\sigma}\right) \right], \quad (\text{A4})$$

and \mathcal{P} denotes the principal value integration. The last term with the principal value integration in Eq.(A1) contains the linear Landau damping term of associated IAW and the Eq.(A1) as a whole accounts for weakly nonlinear IAW with Landau damping. We note that integration in Eq.(A1) is in the form of a convolution integral (with of course the principal value) and can be written as

$$\mathcal{P} \int_{-\infty}^{+\infty} \left(\frac{\partial \phi}{\partial \xi'} \right) \frac{d\xi'}{\xi - \xi'} = \mathcal{P} \left(\frac{1}{\xi} \right) * \left(\frac{\partial \phi}{\partial \xi'} \right), \quad (\text{A5})$$

where $\mathcal{P}(\xi^{-1})$ is the principal value distribution of ξ^{-1} and the star '*' denotes the convolution operation. Taking Fourier transform \mathcal{F} of the above expression and applying convolution theorem, we have

$$\mathcal{F} \left[\mathcal{P} \int_{-\infty}^{+\infty} \left(\frac{\partial \phi}{\partial \xi'} \right) \frac{d\xi'}{\xi - \xi'} \right] = \mathcal{F} \left[\mathcal{P} \left(\frac{1}{\xi} \right) \right] \mathcal{F} \left[\left(\frac{\partial \phi}{\partial \xi'} \right) \right]. \quad (\text{A6})$$

The Fourier transform of the terms on the right hand side can be readily evaluated,

$$\mathcal{F} \left[\mathcal{P} \left(\frac{1}{\xi} \right) \right] = -i\pi \cdot \text{sgn}(k), \quad (\text{A7})$$

$$\mathcal{F} \left[\left(\frac{\partial \phi}{\partial \xi'} \right) \right] = ik \hat{\phi}(k), \quad (\text{A8})$$

where $\hat{\phi}(k)$ is Fourier transform of the function $\phi(\xi)$.

Considering now only the contribution of the Landau damping term, neglecting the nonlinear and the dispersion terms of Eq.(A1), and taking Fourier transform in space and time domain, we obtain the linear dispersion relation with only the Landau damping term as

$$\omega = -i \cdot \tilde{\gamma} \cdot \pi k \cdot \text{sgn}(k) \equiv -i\pi \tilde{\gamma} |k|, \quad (\text{A9})$$

with $(\pi \tilde{\gamma} |k|)$ as the damping rate. Note that the expression for damping rate can also be derived intuitively by comparing the dimensions with that of the dissipation term in a KdV-Burgers equation in a viscous plasma with viscosity coefficient ν

$$\left[\tilde{\gamma} \cdot \mathcal{P} \int_{-\infty}^{+\infty} \frac{\partial \phi^{(1)}}{\partial \xi'} \frac{d\xi'}{\xi - \xi'} \right] = \left[\nu \frac{\partial^2 \phi^{(1)}}{\partial \xi^2} \right], \quad (\text{A10})$$

where the term on the right hand side is the viscous damping term in a KdV-Burgers equation. Note that Eq.(A1) is same as the KdV-Burgers equation with last term replaced by the dissipative damping term. The viscous damping rate of a fluid modeled by the KdV-Burgers equation is given by (νk^2) , with k being the wave number of the associated wave, which is in this case is IAW. So, by dimensional analysis, we have

$$[\nu k^2] \simeq [\tilde{\gamma} k]. \quad (\text{A11})$$

-
- [1] V. I. Karpman, Sov. Phys. Tech. Phys. **8** (1964).
 - [2] A. V. Gurevich and L. P. Pitaevskii, Sov. Phys. JETP **38** (1974).
 - [3] M. A. Hoefer, M. J. Ablowitz, I. Coddington, E. A. Cornell, P. Engels, and V. Schweikhard, Phys. Rev. A **74**, 023623 (2006).
 - [4] I. Ballai, E. Forgács-Dajka, and A. Marcu, Adv. Space Res. **63**, 1472 (2019).
 - [5] A. Y. Wong, D. L. Mamas, and D. Arnush, Phys. Fluids **18** (1975).
 - [6] T. Intrator, N. Hershkowitz, and R. Stern, Phys. Fluids **26**, 1942 (1983).
 - [7] J. L. Cooney, D. W. Aossey, J. E. Williams, M. T. Gavin, H. S. Kim, Y.-C. Hsu, A. Scheller, and K. E. Lonngren, Plasma Sources Sci. Technol. **2**, 73 (1993).
 - [8] L. Grisham and J. Kwan, Nucl. Instrum. Methods Phys. Res. A. **606**, 83 (2009).
 - [9] R. B. White, B. D. Fried, and F. V. Coroniti, Phys. Fluids **15**, 1484 (1972).
 - [10] Y. Nakamura, J. L. Ferreira, and G. O. Ludwig, J. Plasma Phys. **33**, 237 (1985).
 - [11] Y. Nakamura, Plasma Phys. Control. Fusion **41**, A469 (1999).
 - [12] S. K. Sharma and H. Bailung, Phys. Plasmas **17**, 032301 (2010).
 - [13] H. Bailung, S. K. Sharma, and Y. Nakamura, Phys. Plasmas **17**, 062103 (2010).
 - [14] R. F. Pfaff, J. E. Borovsky, and D. T. Young, Geophys. Monogr. Ser. **102** (1998).
 - [15] M. Hirahara, S. Tanaka, H. Kataoka, S. Kasahara, and S. Kubo, Adv. Space Res. **72**, 4934 (2023).
 - [16] A. Sen, S. Tiwari, S. Mishra, and P. Kaw, Adv. Space Res. **56**, 429 (2015).
 - [17] S. Kumar Tiwari and A. Sen, Phys. Plasmas **23**, 022301 (2016).
 - [18] A. S. Truitt and C. M. Hartzell, J. Spacecr. Rockets **57**, 876 (2020).
 - [19] M. Das and M. P. Bora, Phys. Plasmas **32**, 032301 (2025).
 - [20] S. Jaiswal, P. Bandyopadhyay, and A. Sen, Phys. Rev. E **93**, 041201 (2016).
 - [21] D. Chakraborty, A. Biswas, and S. Ghosh, Phys. Plasmas **29**, 122304 (2022).

- [22] H. Sarkar and M. P. Bora, Phys. Plasmas **30**, 083701 (2023).
- [23] K. Kumar, P. Bandyopadhyay, S. Singh, and A. Sen, Phys. Plasmas **31**, 023705 (2024).
- [24] P. Pathak and H. Bailung, IEEE Trans. Plasma Sci. **53**, 2 (2025).
- [25] R. Z. Sagdeev, in *Reviews of Plasma Physics*, edited by M. A. Leontovich, volume 4, page 23, Consultants Bureau, New York, 1966.
- [26] D. J. Korteweg and G. de Vries, Phil. Mag. **39**, 422 (1895).
- [27] V. E. Zakharov, Soviet Phys. JETP **35**, 908 (1972).
- [28] A. Barman and A. P. Misra, Phys. Plasmas **21**, 073708 (2014).
- [29] A. P. Misra, N. C. Adhikary, and P. K. Shukla, Phys. Rev. E **86**, 056406 (2012).
- [30] N. Chakrabarti and S. Ghosh, Phys. Scripta **97**, 095603 (2022).
- [31] J. W. VanDam and T. Taniuti, J. Phys. Soc. Jpn. **35**, 897 (1973).
- [32] T. Matsoukasa and M. Russell, J. Appl. Phys. **77**, 4285 (1995).
- [33] I. Hutchinson, *Principles of Plasma Diagnostics*, Cambridge University Press (CUP), 2002.
- [34] D. Hastings and H. Garrett, *Spacecraft-Environment Interactions*, Cambridge University Press (CUP), 2004.
- [35] W. J. Raitt, Adv. Space Res. **7**, 179 (1987).
- [36] S. Jaiswal, P. Bandyopadhyay, and A. Sen, Phys. Rev. E **93**, 041201 (2016).
- [37] J. P. Boris and D. L. Book, J. Comput. Phys. **11**, 38 (1973).
- [38] S. T. Zalesak, J. Comput. Phys. **31**, 335 (1979).
- [39] Y. Nakamura, H. Bailung, and Y. Saitou, Phys. Plasmas **11**, 3925 (2004).